2014

Omnidirectional Microstrip Patch Antenna with Reconfigurable Pattern and Polarisation

Max Ammann
Technological University Dublin, max.ammann@tudublin.ie

Xiulong Bao
Technological University Dublin, xiulong.bao@tudublin.ie

Adam Narbudowicz
Technological University Dublin, adam.narbudowicz@mydit.ie

Recommended Citation

Narbudowicz, A., Bao, X. & Ammann, M. (2014) Omnidirectional microstrip patch antenna with reconfigurable pattern and polarisation. *IET Microwaves, Antennas & Propagation*, Vol. 8, Issue 11. 2014, Pg. 872-877. doi:10.1049/iet-map.2013.0665

Omnidirectional microstrip patch antenna with reconfigurable pattern and polarisation

Adam Narbudowicz [a] *{adam.narbudowicz@mydit.ie},*
Xiulong Bao [b] *{xbao@dit.ie},*
Max J. Ammann [b] *{max.ammann@dit.ie}*

[a] *CTVR - The Telecommunication Research Centre,*
Trinity College Dublin,
Dunlop Oriel House,
Dublin 2, Ireland

[b] *Antenna & High Frequency Research Centre,*
Dublin Institute of Technology,
Kevin Street
Dublin 8, Ireland

Abstract: An omnidirectional microstrip patch antenna, capable of reconfiguring both polarisation and radiation pattern is proposed. It operates with two orthogonal ±45° slanted linear polarisations and can produce two dipole-like radiation patterns, providing 360° coverage in either the horizontal or elevation plane. With appropriate steering, this enables a single antenna to provide full spherical coverage for any polarisation. The reconfiguration is realised by phase shifting, thus does not require switching elements, such as MEMS or pin diodes embedded into antenna. The basic principles of operation are discussed and validated by numerical and measured data.

1. Introduction

The capability of an antenna to receive or transmit signals for any arbitrary angle over a full sphere is highly desirable for many radio applications, such as point to multipoint transmission, RFID detection or sensing. Isotropic antennas, as proved by Mathis [1] are impossible to realise due to the mathematical properties of a continuous vector field tangential to a sphere (as seen in far field radiation pattern). To overcome this difficulty,

some antennas offer full spherical coverage using reconfigurable antennas [2-5] or integrated multi-port antennas with different radiation patterns [5-8].

In the first category, Zhang *et al.* [2] proposed a reconfigurable antenna consisting of two symmetrical elements, which can swap the role of radiator and reflector. The resultant antenna offers two oppositely directed modes. The antenna operates over a large bandwidth, however the impact of the switches and its steering on antenna performance is not reported. Reconfigurable antennas employing *pin* diodes to switch the beam either in elevation and azimuth [3] or sweeping it over 360°in the azimuth plane [4] are reported. Both approaches focused on selective beams, and do not provide full spherical coverage. In [5] a pattern and frequency reconfigurable antenna offers two different radiation patterns, steered by two switching elements.

The multiport antenna approach can provide better spherical coverage, however at the price of expensive additional transceivers needed to process the signal. In [6] a compact antenna is proposed, which integrates a dual-polarised patch, a monopole and a quasi-loop antenna. This approach allows coverage of most signals within a full sphere (with the exception of direction obstructed by the ground plane) and with two orthogonal polarisations. Another approach by Martens and Manteuffel [7] uses characteristic modes on a ground plane to provide a two port MIMO antenna covering all angles around a sphere. Since the ground plane acts here as a radiator, the antenna covers a very wide range of angles around a full sphere, however the polarisation issues are not investigated. In [8] a four-feed antenna is proposed, capable of producing either a linearly-polarised conical beam or a circularly-polarised beam on boresight. Finally [9] proposes a circularly polarised antenna with a dipole-like radiation pattern that can be rotated. The solution also offers full spherical coverage, however covers only a single polarisation (RHCP).

In this paper we propose an antenna, capable of radiating two orthogonal linear ±45° slanted polarisations, each with two dipole-like patterns: one covering 360° in horizontal plane, and the other in the elevation. This, when combined with proper steering, allows coverage of any polarisation from any arbitrary angle in a sphere. The switching between antenna configurations is realized by different phase excitation at the four antenna ports. There are no switching components integrated into antenna. To steer the antenna beam and polarisation, any state of the art method providing a sufficient phase shift can be used, such as tunable capacitors, reconfigurable couplers [10], liquid crystal delay line etc. For measurements conducted in this paper the reconfigurable element was emulated by a rat-race coupler, which provided 0° and 180° phase shifts. Also, with this coupler, multiple antenna modes can be used at the same time. This is an important advantage for many point-to-multiport radio systems.

This paper is organized as follows: section 2 provides a description of the proposed antenna; section 3 explains the principles of operation; section 4 investigates the proposed antenna with idealized feeds; section 5 presents simulated and measured results; finally conclusions are provided in section 6.

2. Antenna design

The antenna comprises two back-to-back coupled patches [11], which share a common ground plane as seen in Fig. 1. It has three metallization layers, milled on a Taconic RF-35 substrate. Each substrate layer is 1.5 mm high, with a relative permittivity $\varepsilon_r = 3.47$. In the prototyping process the two layers are milled separately, each with its own ground plane. Next four SMA connectors are soldered, two to each layer. The layers are then joined

together, providing good electrical contact between both ground planes and effectively merging them into single metallization layer.

The patches are rectangular and are fed from microstrip lines connected to the two lower corners. They operate at a basic resonance frequency of 2.56 GHz. Since the antenna is based on a simple rectangular patch resonator, it can be easily tuned in frequency by varying parameters L_p and L_q. Two feeds for each patch are required in order to achieve dual linear ±45° slanted polarisation. For pattern reconfigurability, the electric field must be excited along all four edges of each patch. To achieve this, each patch is fed at a corner. Although this technique is usually applied for circularly polarised antennas, here it realises a linear slanted polarisation as both the length and width of the patch are equal. A significant problem is very high input impedance at the corner. Considering this, two measures were undertaken to provide a good match: the corners, at which each patch is fed, were truncated by Δs = 5 mm to decrease the input impedance; also quarter-wavelength transformers (which are 0.3 mm wide and have impedance Z = 142Ω) were implemented. The 50Ω microstrip lines were traced into the edge of the PCB, where SMA connectors were soldered. The antenna dimensions are: W_s = 42 mm; L_s = 5 mm; W_g = 5.5 mm; L_g = 5.5 mm; L_p = 31 mm; L_q = 16 mm; Δ_s = 5 mm.

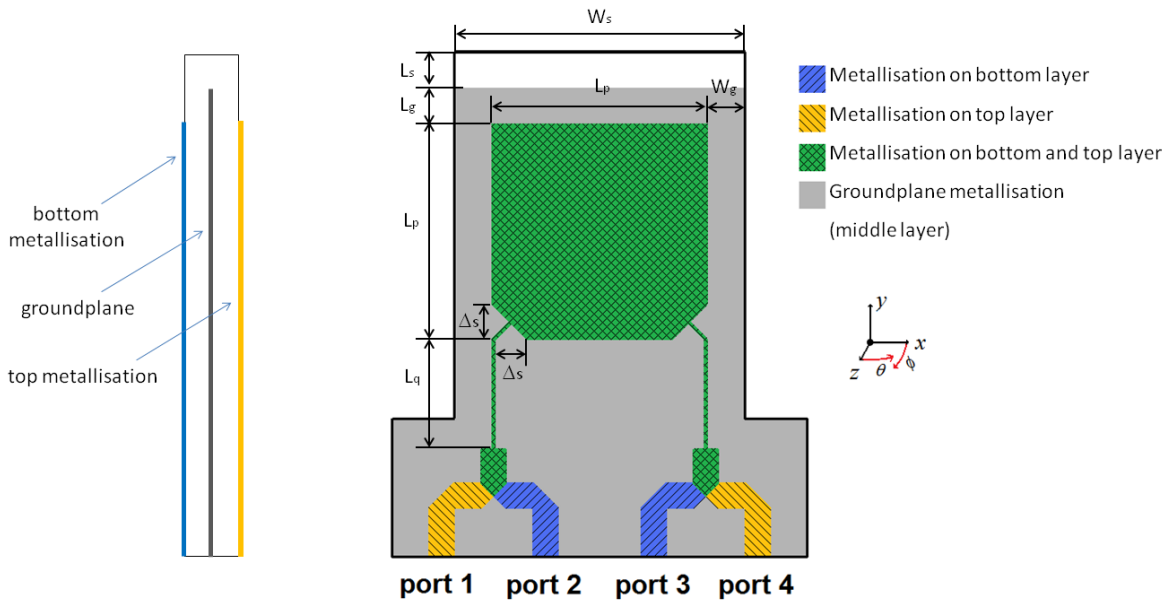

Fig. 1 Geometry of the proposed antenna: side view (left) and front view with important dimensions (right).

The antenna has four input ports (two for each of the back-to-back coupled patches). The pattern reconfigurability is implemented by a phase difference between the ports and polarisation is determined by port selection. The investigated configurations are listed in Table 1. It can be seen, that each configuration excites only two of four ports. The change of the excited ports determines the polarisation, i.e. if ports 1 and 3 are excited, the antenna produces +45° slanted polarisation, whereas for ports 2 and 4 it is -45 slanted polarisation. The excited ports are either in-phase (i.e. 0° phase difference) or out-of-phase (i.e. 180° phase difference). This enables rotation of the dipole-like pattern by 90° around *z*-axis. Fig. 2 shows a photo of the prototyped antenna, with the rat-race coupler [12] attached to achieve proper configuration.

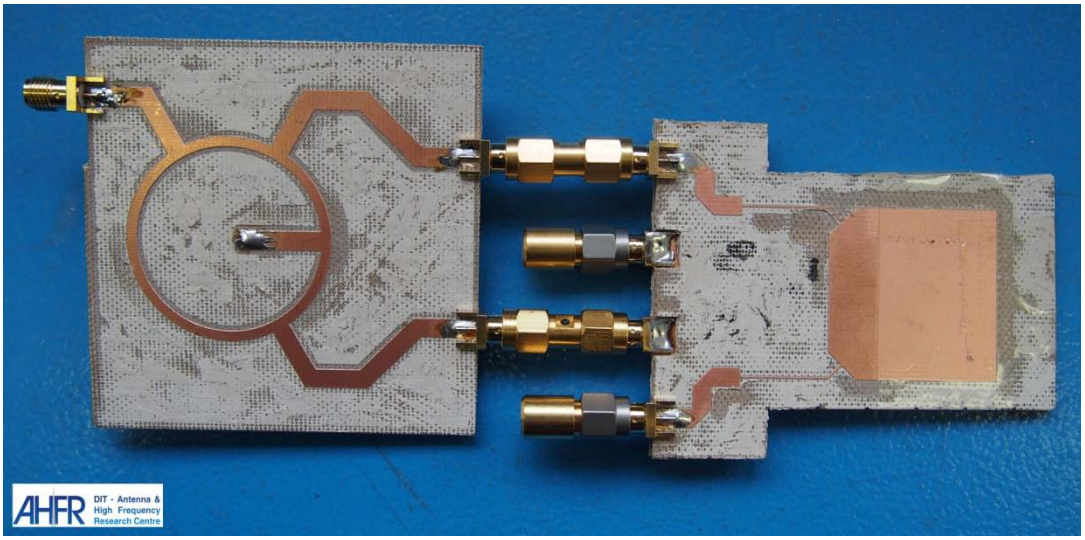

Fig. 2 Photograph of the prototyped antenna with the rat-race coupler used in measurement and simulation. The coupler as seen here realizes configurations A and B. Unused ports are terminated with a 50Ω match.

3. Principles of operation

In order to explain the principles of operation, the electric field for each edge is investigated. Fig. 3 depicts the electric fields in the top and bottom patch for the four configurations mentioned in Table 1. The method relies on the superposition of the electric fields, produced by four edges of each patch. This requires two orthogonal modes of the patch (TM_{100} and TM_{010}) to be excited, hence the use of a corner feed. Configurations A and B excite feeds located in the left lower corner (i.e. ports 1 and 3), therefore the superposition of the four edges produce +45° slanted polarisation (please note, that bottom patch is shown from +*z* direction, however it produces main radiation in -*z* direction). Similarly, the configurations C and D excite feeds located in the right lower corner (i.e. ports 2 and 4), producing -45° slanted polarisation. In order to demonstrate how to switch the plane in which the radiation is produced, the phase difference between the corresponding edges of the top and bottom patch are investigated. Generally, since the patches are in a back-to-back orientation, a phase difference of 0° means the electric field vectors are oriented in the

opposing directions, therefore producing a null in the radiation pattern. However a phase difference of 180° means the electric field vectors are aligned in the same direction and radiation is produced.

Configuration	Polarisation	Plane of radiation	Phase at port:			
			1	2	3	4
A	+45°	*xz*	0°	X	0°	X
B	+45°	*yz*	0°	X	180°	X
C	-45°	*xz*	X	0°	X	0°
D	-45°	*yz*	X	0°	X	180°

Table 1: The four antenna configurations and the corresponding port phases, polarisation and plane in which the omnidirectional radiation pattern is produced. X means there is no excitation at the given port.

Feeding the antenna ports with different phase shifts results in a change of the phase shift between the edges of the patch (i.e. between the corresponding edges of top and bottom patch). This relationship is demonstrated in Fig. 3. For instance, in configuration A the two patches are fed in phase. This causes the edges in ±*y* directions to be also in phase, resulting in a null for this direction. However the edges in the ±*x* directions are out of phase, interfering constructively and producing radiation. As a consequence configuration A will produce a +45° polarisation with an omnidirectional radiation pattern in the horizontal plane (i.e. *xz*-plane) and nulls in ±*y* directions. Configuration C will produce the same radiation pattern with -45° polarisation.

If the top and bottom patches are fed out-of-phase (as in configurations B and D), the edges in the ±*x* directions are in phase, producing nulls, and the edges in ±*y* directions are out of phase, radiating in the *yz*-plane. It should be noted that this mode is much more challenging as the radiation is produced in the plane where the feeds are located. This causes

ripples in the radiation pattern and degraded the polarisation purity in the -*y* directions ($\theta = 90°$) where the feeds and steering circuitry are located.

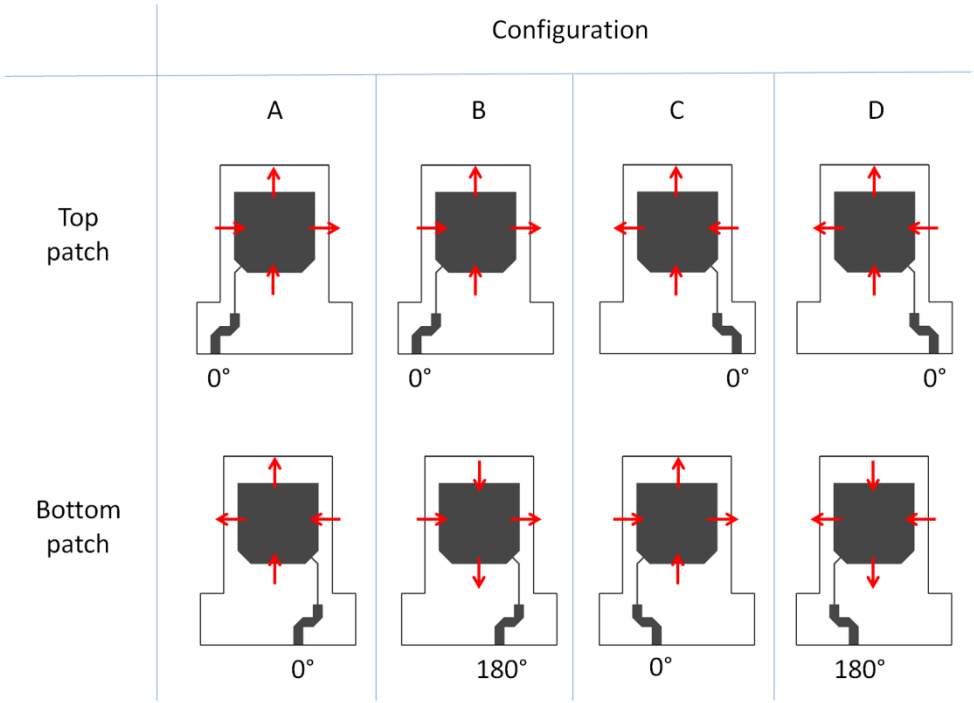

Fig. 3 The electric field for each patch, shown for the four configurations described in Table 1. Non-excited ports are removed for clarity and the bottom patch is viewed from the top through the substrates.

4. Idealized model

The antenna was first simulated with idealized excitations, i.e. the signals with desired phase shift were applied directly at the antenna ports (ignoring the impact of feed network). For this purpose a time-domain solver of CST Microwave Studio was used [13]. Fig. 4 presents simulated realized gains for configurations A and B. It can be seen, that the plots exhibit good dipole-like radiation pattern with one plane being omnidirectional (i.e. plane *xz* for configuration A and plane *yz* for configuration B) and the other being figure-of-eight shape (i.e. plane *yz* for configuration A and plane *xz* for configuration B) with two distinctive nulls. The squint visible in yz-plane for configuration A is most likely due to the microstrip

lines and quarter wavelength transformers. The results for configurations C and D are similar (with the change of dominant polarisation) and hence not shown for brevity.

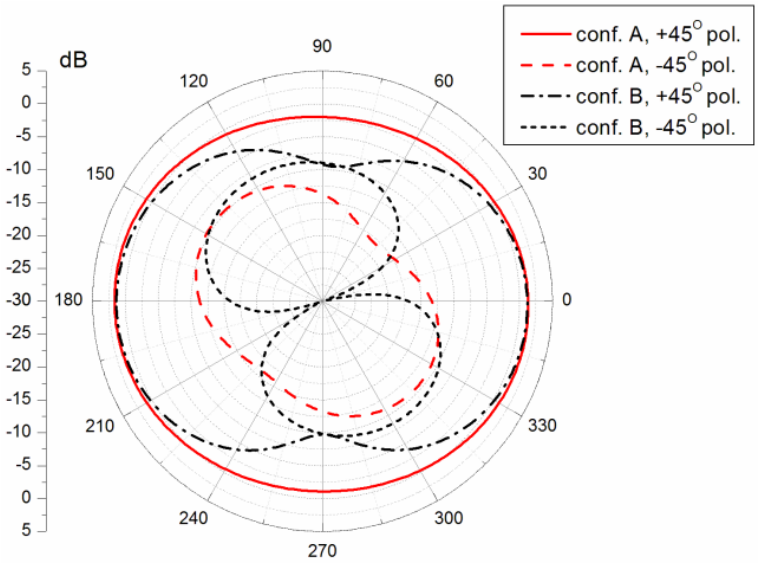

a)

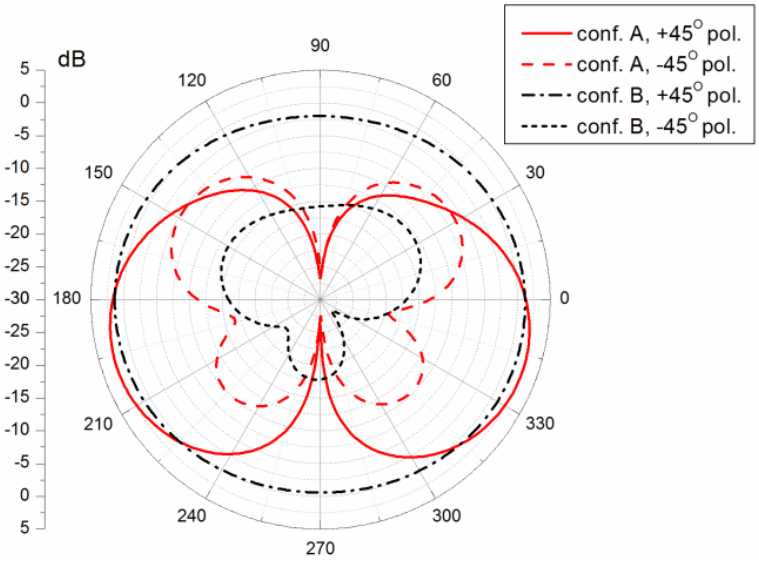

b)

Fig. 4 Simulated realized gains for antenna with idealised rat-race coupler. a) *xz*-plane; b) *yz*-plane.

This configuration is in fact similar to the intended commercial application, where the antenna will be fed from an integrated transceiver. However for the laboratory measurements an external steering network was required to switch the antenna configuration. For this a rat-race coupler (as seen on Fig. 2) was used both in measurement and simulation. Also a feed

cable was attached to connect the antenna under test with measurement equipment. The cable is attached in *yz*-plane at $\theta = 90°$, i.e. at a location where a radiation is produced in configurations B and D. This perturbs the radiation pattern measurement [14] and is visible as ripples in the radiation patterns, as well as decreased polarisation purity (in comparison to simulated results) for some angles in configurations B and D.

5. Results

Fig. 5 depicts simulated and measured reflection coefficients S_{nn} for each of the four antenna ports. It can be seen, that the results are in a reasonable agreement, but with a minor shift towards higher frequencies for the prototyped antenna. Also in the simulated results, a very small shift can also be seen between the ports located on top layer (i.e. ports 1 and 4) and bottom layer (i.e. ports 2 and 3). This is not seen in the measured data, as prototyping inaccuracies have a greater dominating effect. The isolation between ports is greater than 15 dB and hence is not shown for clarity. The radiation patterns for various configurations are shown in the following sections. All measured data is shown for 2.56 GHz and simulated for 2.55 GHz.

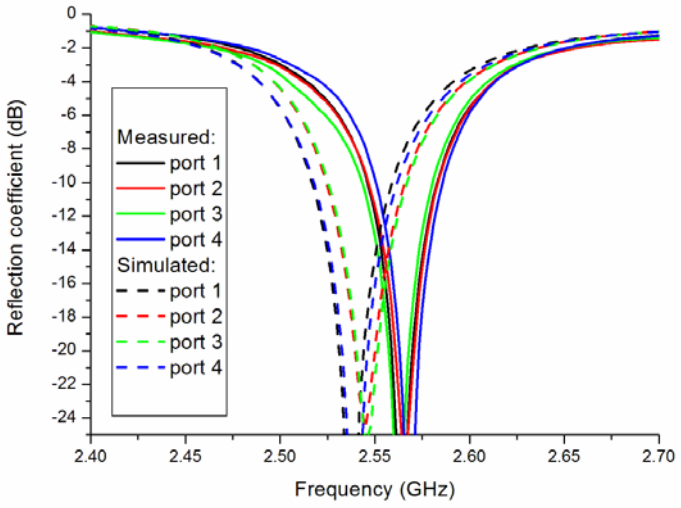

Fig. 5 Measured and simulated reflection coefficients of the proposed antenna

Configuration A

Fig. 6 presents the realized gains for the proposed antenna in configuration A. It can be seen, that the omnidirectional coverage was produced in *xz*-plane. Unlike in Fig. 4, the ripples can be seen in *yz*-plane, which are the effect of feed cable and rat-race coupler. The simulation in CST Microwave Studio incorporated the coupler and a good agreement is achieved between measurement and simulation. The measured gain for +45° polarisation in *xz*-plane varies between 2.7 dBi and -0.7 dBi. In this plane the cross polarisation level (i.e. -45°) is better than 11 dB.

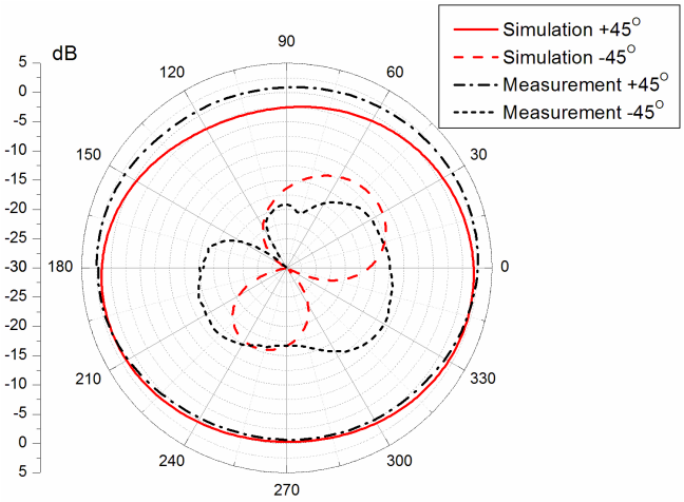

a)

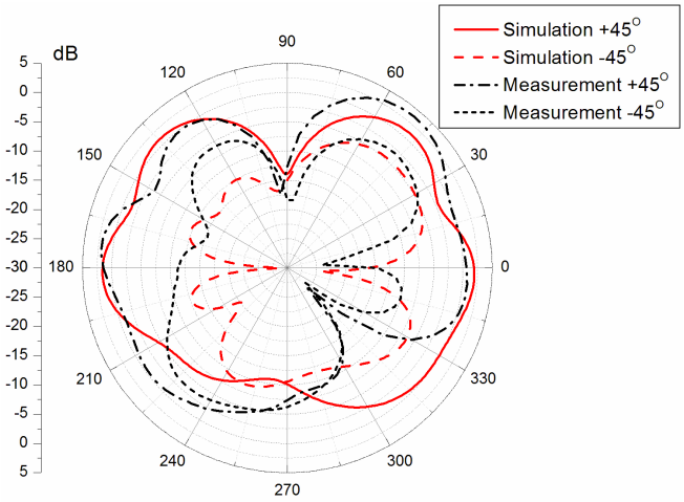

b)

Fig. 6 Realized gains for the proposed antenna in configuration A. a) *xz*-plane; b) *yz*-plane.

Configuration B

Fig. 7 presents the realized gains for the proposed antenna in configuration B. It can be seen, that the 180° phase difference between ports 1 and 3 produced omnidirectional radiation in *yz*-plane and a shape-of-eight pattern with two distinctive nulls. This is similar radiation pattern, as expected from a dipole antenna. The figure-of-eight is more apparent for this configuration, as the *xz*-plane is more resilient to distortion caused by reflection from the feed cables and coupler. A deterioration of the measured polarisation purity can however be seen in *yz*-plane for angles θ = 90° and θ = 270°, compared to the simulated results. This is caused by reflection from the feed cable, which is mounted in this plane at θ = 90°. The maximum measured realized gain is 3.2 dBi and degrades to -5.7 dBi at θ = 90°, i.e. location where the feed cable is mounted. The simulated results, which include the effect of the coupler but not the feed cable, are 2.2 dBi and -3.5 dBi respectively. The measured cross polarisation level in the *yz*-plane is better than 10 dB for angles θ from 125° to 255° and from 295° to 60°.

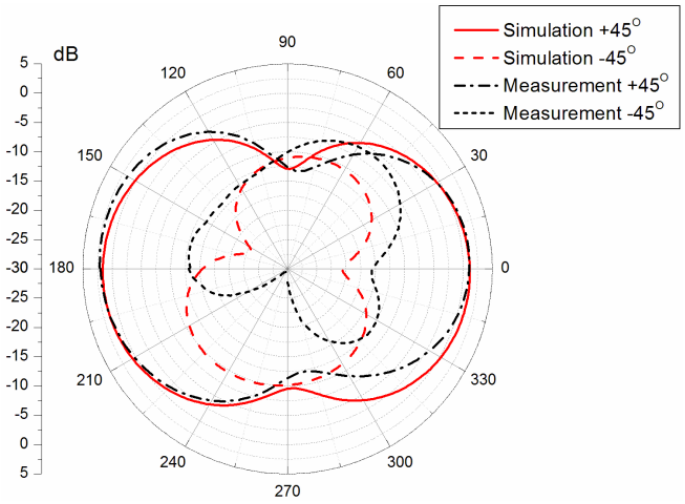

a)

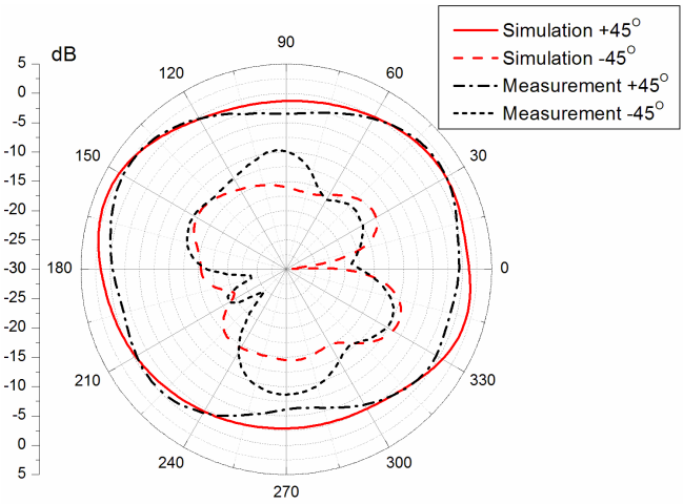

b)

Fig. 7 Realized gains for the proposed antenna in configuration B. a) *xz*-plane; b) *yz*-plane.

Configuration C

Fig. 8 presents the realized gains for the proposed antenna in configuration C. Similar to configuration A, the omnidirectional radiation pattern is produced in *xz*-plane, however the dominant polarisation is -45°. The measured realized gain in *xz*-plane varies between 2.1 dBi and -2.4 dBi. The measured cross polarisation level in the whole *xz*-plane is better than 9.5 dB.

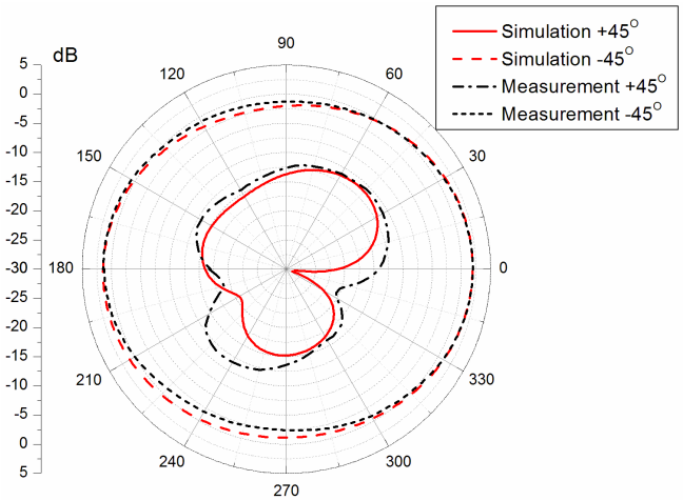

a)

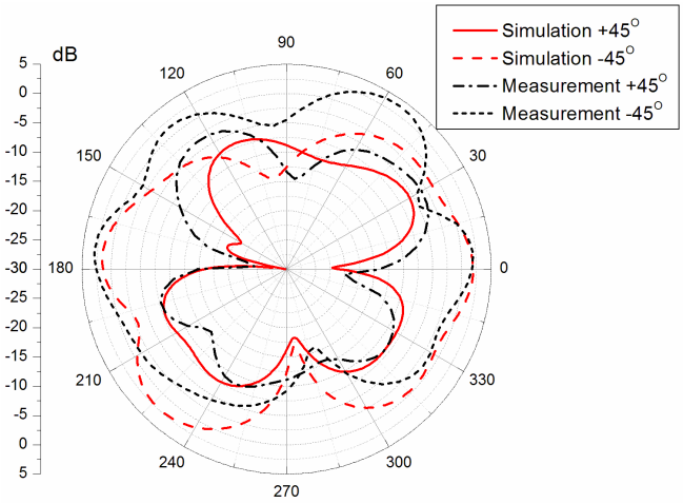

b)

Fig. 8 Realized gains for the proposed antenna in configuration C. a) *xz*-plane; b) *yz*-plane.

Configuration D

Fig. 9 presents the realized gains for the proposed antenna in configuration D. The dominant polarisation is -45° and the omnidirectional pattern is produced in the *yz*-plane, with the two distinctive nulls and a figure-of-eight shape in *xz*-plane. Also here, the effect of the feed cable reflection is visible in the *yz*-plane as decreased polarisation purity for θ = 90° and θ = 270°. Measured realized gain in the *yz*-plane varies between 3.4 dBi and -4 dBi, with simulated gain of 2.1 dBi and 4.3 dBi. The measured cross polarisation level in *yz*-plane is better than 10 dB for angles θ from 115° to 255° and from 300° to 55°.

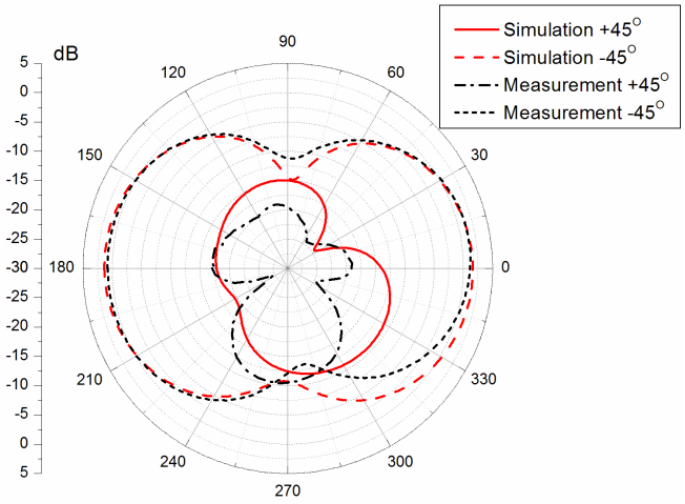

a)

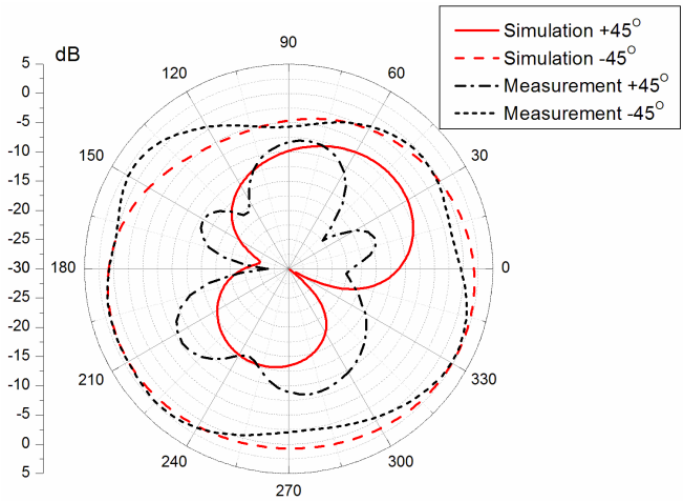

b)

Fig. 9 Realized gains for the proposed antenna in configuration D. a) *xz*-plane; b) *yz*-plane.

6. Conclusions

The proposed antenna offers a high degree of pattern and polarisation reconfigurability. Two slanted linear polarisation of ±45° are provided, each with two dipole-like radiation patterns. Using proper steering, allows reception or transmission of signals of any polarisation, from any arbitrary spherical angle. The antenna does not incorporate any switching components, avoiding inter-modulation issues and simplifying the design. It also allows two configurations to be used at the same time, which is beneficial for MIMO

applications. The basic principles of operation were successfully validated. The antenna is proposed for combating multipath fading for indoor wireless propagation scenarios.

References:

[1] H. F. Mathis, “A short proof that an isotropic antenna is impossible,” *Proceedings of the IRE,* vol. 39, issue 8, pp. 970, Aug. 1951.

[2] G.-M. Zhang, J.-S. Hong, G. Song, and B.-Z. Wang, "Design and analysis of a compact wideband pattern-reconfigurable antenna with alternate reflector and radiator", *IET Microwaves, Antennas and Propagation,* vol. 6, issue 15, pp. 1629 - 1635, Dec. 2012.

[3] S. V. Shynu, and M. J. Ammann, "Reconfigurable Antenna With Elevation and Azimuth Beam Switching", *IEEE Antennas and Wireless Propagation Letters*, vol. 9, pp. 367 - 370, 2010.

[4] Y.-Y. Bai, S. Xiao, M.-C. Tang, C. Liu, and B.-Z. Wang, "Pattern reconfigurable antenna with wide angle coverage", *Electronics Letters*, vol. 47, issue 21, pp. 1163 - 1164, Oct. 2011.

[5] I. Shoaib, S. Shoaib, X. Chen, and C. Parini, " A Single-Element Frequency and Radiation Pattern Reconfigurable Antenna ", Proc.: *EuCAP - European Conference on Antennas and Propagation*, Gothenburg, Sweden, pp. 2057 - 2060, Apr. 2013.

[6] D. Heberling, and C. Oikonomopoulos-Zachos, "Multiport antennas for MIMO-systems", Proc.: *LAPC - Loughbourough Antennas & Propagation Conference,* Loughborough, UK, pp. 65-70, Nov. 2009.

[7] R. Martens, and D. Manteuffel, "2-Port Antenna Based on the Selective Excitation of Characteristic Modes", Proc.: *APSURSI - Antennas and Propagation Society International Symposium,* Chicago, USA, Jul. 2012.

[8] W. Cao, B. Zhang, A. Liu, T. Yu, D. Guo, and K. Pan, “A reconfigurable microstrip antenna with radiation pattern selectivity and polarisation diversity”, *IEEE Antennas and Wireless Propagation Letters*, vol. 11, pp. 453 - 456, Apr. 2012.

[9] A. Narbudowicz, X. L. Bao, M. J. Ammann, H. Shakhtour, and D. Heberling, "Circularly Polarized Antenna with Steerable Dipole-like Radiation Pattern", *IEEE Transactions on Antennas and Propagation*, vol. 62, issue 2, pp. 519-526, Feb. 2014.

[10] F. Ferrero, C. Luxey, R. Staraj, G. Jacquemod, M. Yedlin, and V. Fusco, “Theory and design of a tunable quasi-lumped quadrature coupler”, *Microwave and Optical Technology Letters*, vol. 51, no. 9, pp. 2219 - 2222, Sep. 2009.

[11] H. Iwasaki, "A back-to-back rectangular-patch antenna fed by a CPW", *IEEE Transactions on Antennas and Propagation*, vol. 46, issue 10, pp. 1527-1530, Oct. 1998.

[12] D. M. Pozar, "Microwave Engineering", 2ed., John Wiley & Sons, 1998, pp. 401 - 407.

[13] "CST Microwave Studio - Workflow & Solver Overview", CST - Computer Simulation Technology AG, 2013.

[14] D. Manteuffel, and R. Martens, "Improved Radiation Pattern Measurements of MIMO Handheld Mobile Terminals", Proc.: 7th European Conference on Antennas and Propagation, EuCAP 2013, Goteborg, Sweden, Apr. 2013.